*Paper 106*

# Borehole Resistivity Logging and Tomography for Mineral Exploration

Qian, W. [2,1], Milkereit, B. [1], McDowell, G. [3], Stevens, K. [4], Halladay, S. [5]

1. Dept. of Physics, University of Toronto, Canada
2. Geoserve Logging & Tomography
3. CVRD Inco Technical Services Ltd.
4. Xstrata Nickel Ltd.
5. First Nickel Ltd.

**ABSTRACT**

*This paper focuses on the use of cross-borehole electric methods in ore body delineation. A BRT (Borehole Resistivity Tomography) test survey has been conducted to map massive sulfide zones between boreholes up to 130 m apart. The boreholes need to be water filled, so as the electrode array couples to the rock formation. We have established a multi-step procedure for data acquisition, processing and interpretation. Between boreholes, we have successfully imaged the massive sulfide mineralization in a very resistive host. We have demonstrated that the equipment is easy to deploy in water filled boreholes and we conclude that single borehole Vertical Resistivity Profiling (VRP) data can detect conductive zones within a 30 m range around the borehole and it also provides an independent estimate of bulk (4 - 100 m) resistivity for calibration / interpretation of other EM datasets. The cross-borehole tomography data can map conductive zones between boreholes up to 130 m apart. We did not test the larger offset during the present experiments.*

## INTRODUCTION

Electric resistivity surveying along the earth's surface is a well-known geophysical exploration technique. Due to its conceptual simplicity, low equipment cost and ease of use, the method is routinely used in mineral exploration. Borehole resistivity tomography, in which both current electrodes and potential electrodes are placed in two boreholes, can provide detailed information about resistivity distribution between the boreholes (Daniels 1977; Daniels and Dyck 1984; Shima 1992). Daniels and Dyck (1984) demonstrated a variety of applications of borehole resistivity measurements to mineral exploration. Unfortunately these early case histories didn't include an inversion of the data. Conventional mise-a-la-masse types of measurements are carried out by placing a current electrode in a conductive zone and measuring the potential field distribution in one or more boreholes (Mwenifumbo, 1997). Recently, with enhanced computing resources, there has been increasing interest to construct tomographic images through geophysical inversions (Loke and Barker, 1995, 1996). However, smoothness constraint OCCAM type of inversion often yield unsatisfactory results, particularly when there are large contrasts in the resistivity model, a situation often encountered in mineral exploration.

During the fall of 2006, we collected several single borehole Vertical Resistivity Profiling (VRP), borehole-to-borehole, and borehole-to-surface resistivity tomography (BRT) data sets across several different massive sulfide deposits. Here we report results from data collected in the Sudbury basin, Ontario, Canada. The boreholes were water filled and borehole to borehole separation varied from 40 m to 130 m. The data acquisition system was developed by Geoserve in Germany for near surface archaeological and hydrological applications. What is unique about the borehole resistivity system is its electrode and borehole cable design, which allow seamless integration of borehole and surface measurements. The use of borehole cables with up to 24 electrodes each allows the system to acquire more than one thousand resistance readings per hour. Each borehole cable can be carried around by an All Terrain Vehicle (ATV) or two people; data acquisition unit allows real time data Quality Control (QC); pre-programmed data acquisition procedures allow the full waveform data stored in binary files, which can be converted to ASCII files easily. The data acquisition geometries are shown in Figure 1. The configuration for cross borehole resistivity tomography was proposed by Zhou and Greenhalgh (2000). In this configuration, the current electrodes and potential electrodes straddle the two boreholes. Very clean waveform data has been acquired for both configurations (Figure 1 d-e). In this paper, we follow the popular convention and use “A” to denote the positive current electrode, “B” the negative current electrode, “M” the positive potential electrode and “N” the negative potential electrode.

In "Proceedings of Exploration 07: Fifth Decennial International Conference on Mineral Exploration" edited by B. Milkereit, 2007, p. 1115-1118

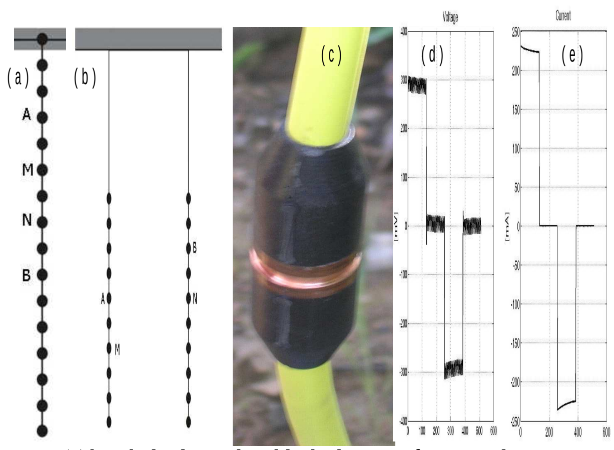


**Figure 1:** (a) borehole electrode cable deployment for vertical resistivity profiling; (b) cross borehole tomography; (c) copper-ring electrode; (d) measured voltage waveform; and (e) injected current waveform for 130 m electrode separation between boreholes.

## APPARENT RESISTIVITY FORMULATION

Apparent resistivity is an excellent parameter for data display and quality control, because the geometrical factor and ground surface effect have been removed from apparent resistivity formulation. The apparent resistivity values reflect the weighted volume averaging of true earth resistivity in a region defined by current electrodes A, B and potential electrodes M, N.

In a homogenous half space, we inject a current "I" between points A and B and measure the potential difference between points M and N. Due to the "mirror" effect of the ground surface as shown in Figure 2, the potential at point (x, z) is:

$$u(x,z) = \frac{\rho I}{4\pi}\left(\frac{1}{r_1}+\frac{1}{r_2}-\frac{1}{r_3}-\frac{1}{r_4}\right)$$

$$= \frac{\rho I}{4\pi}\left(\frac{1}{\sqrt{(x-x_A)^2+(z-z_A)^2}}+\frac{1}{\sqrt{(x-x_A)^2+(z+z_A)^2}}-\frac{1}{\sqrt{(x-x_B)^2+(z-z_B)^2}}-\frac{1}{\sqrt{(x-x_B)^2+(z+z_B)^2}}\right)$$

where ρ is the resistivity of the half space.

The potential difference between points M and N is:

$$\Delta u_{MN} = \frac{\rho I}{4\pi}\left(\frac{1}{r_{MA!}}+\frac{1}{r_{MA2}}-\frac{1}{r_{MB1}}-\frac{1}{r_{MB2}}-\frac{1}{r_{NA!}}-\frac{1}{r_{NA2}}+\frac{1}{r_{NB1}}+\frac{1}{r_{NB2}}\right)$$

Therefore the apparent resistivity is:

$$\rho_a = \frac{4\pi}{\frac{1}{r_{MA!}}+\frac{1}{r_{MA2}}-\frac{1}{r_{MB1}}-\frac{1}{r_{MB2}}-\frac{1}{r_{NA!}}-\frac{1}{r_{NA2}}+\frac{1}{r_{NB1}}+\frac{1}{r_{NB2}}}\frac{\Delta u_{MN}}{I} = k\frac{\Delta u_{MN}}{I}$$

Where the geometric factor k is:

$$k = \frac{4\pi}{\frac{1}{r_{MA!}}+\frac{1}{r_{MA2}}-\frac{1}{r_{MB1}}-\frac{1}{r_{MB2}}-\frac{1}{r_{NA!}}-\frac{1}{r_{NA2}}+\frac{1}{r_{NB1}}+\frac{1}{r_{NB2}}}$$

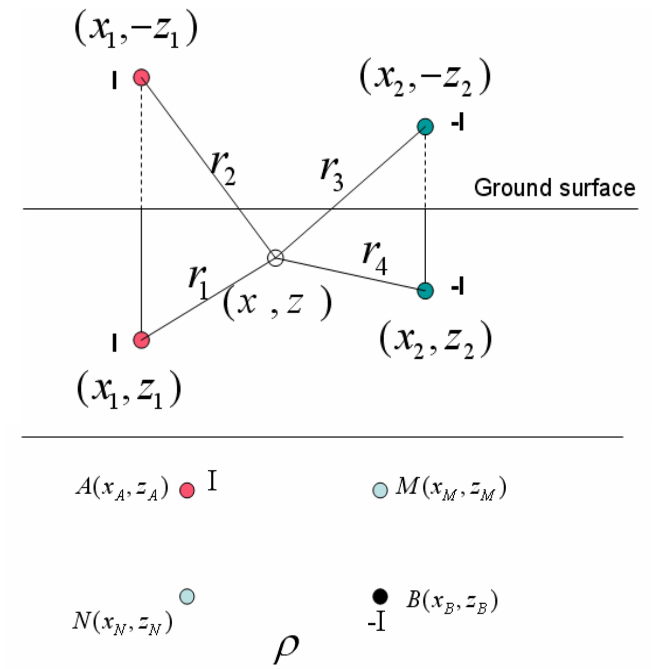


$$r_{MA1} = \sqrt{(x_M - x_A)^2 + (z_M - z_A)^2}$$
$$r_{MA2} = \sqrt{(x_M - x_A)^2 + (z_M + z_A)^2}$$
$$r_{MB1} = \sqrt{(x_M - x_B)^2 + (z_M - z_B)^2}$$
$$r_{MB2} = \sqrt{(x_M - x_B)^2 + (z_M + z_B)^2}$$
$$r_{NA1} = \sqrt{(x_N - x_A)^2 + (z_N - z_A)^2}$$
$$r_{NA2} = \sqrt{(x_N - x_A)^2 + (z_N + z_A)^2}$$
$$r_{NB1} = \sqrt{(x_N - x_B)^2 + (z_N - z_B)^2}$$
$$r_{NB2} = \sqrt{(x_N - x_B)^2 + (z_N + z_B)^2}$$

Figure 2: Mirroring effect of the ground surface for potentials measured at points M and N.

## VERTICAL RESISTIVITY PROFILING (VRP)

From the electrode array in a single borehole, we perform Vertical Resistivity Profiling (VRP), in which the current and potential electrode setup is the same as surface Schlumberger survey. The measured voltages are converted into apparent resistivity through a geometry factor, which takes into account the earth-air surface. The apparent resistivity pseudo-section is created by assigning the apparent resistivity at AB/2 away from the borehole. The VRP data can usually be collected within half an hour. In the following, we will discuss VRP data characteristics for two different situations.

### Borehole intersects the sulfide zone

An example of VRP apparent resistivity pseudo-section for this case is shown in Figure 3, in which we can clearly identify that the sulfide zone has an apparent resistivity of less than 50 ohm.m. This zone is located between the depths of 40 and 50 m and its lateral extension is more than 30 m. From this pseudo-section, we can see that there is a tinge of a weak conductor about 10 m away from the borehole at the depth of 25 m. This thin zone does not seem to be in contact with the borehole.

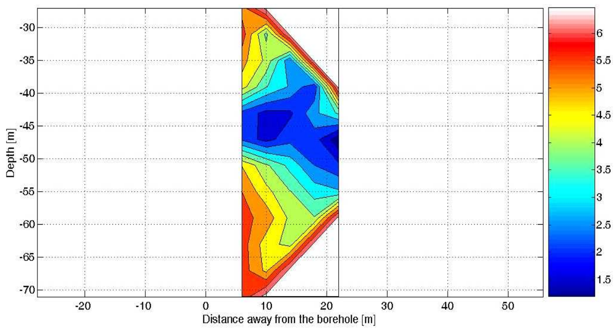


**Figure 3:** VRP apparent resistivity pseudo-section for a borehole which intersects massive sulfides at the depth of 40 – 50 m.

### Borehole pass by a sulfide zone at a distance

An example of VRP apparent resistivity pseudo-section for this case is shown in Figure 4. We can see that there is a conductive zone at the depth of 60-70 m. This zone is about 10 m away from the borehole. However, from the measurements in a single borehole, we can not determine the azimuth (direction) of this extension. Surface electrode lines must be deployed for the determination of the azimuth. VRP has another advantage in that it provides bulk resistivity measurements. Conventional resistivity logging provides resistivity readings on a scale of tens of centimeters, while VRP measures bulk resistivity on a scale of ~ 10 m. Although the borehole induction electromagnetic methods are sensing bulk resistivities, they have no resolution for resistive and moderately resistive formations. VRP resistivity data can be used for calibration / interpretation of other EM datasets.

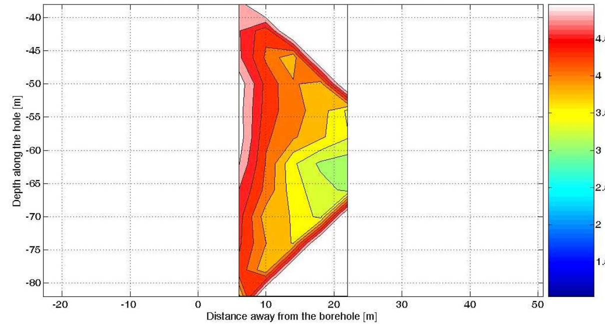


**Figure 4:** VRP apparent resistivity pseudo-section for a borehole which passes a massive sulfide ore body at a distance. From this pseudo-section, we can see that a massive sulfide zone is about 15 m away from the borehole at the depth of 60-70 m. Note the decreasing apparent resistivity with large offset.

### CROSS BOREHOLE ELECTRIC CURRENT MAPPING – A QUALITY CONTROL TOOL

When a constant injection voltage is applied between electrodes A and B across the two boreholes, the electric current flowing between A and B depends on the contact resistances of electrodes A and B, and the rock formation resistance from A to B. If the borehole is water filled, we can assume the contact resistance is uniform. Thus the electric current from A to B maps the rock formation resistance between points A and B. An example of the electric current between A and B is shown in Figure 5. Note the data shows characteristics of two conductive zones (marked I and II in Figure 5) between the two boreholes. The borehole separation is 48 m.

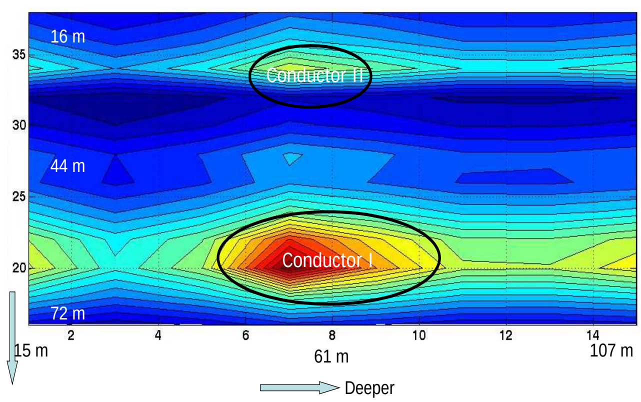


**Figure 5:** Quality control of electric current flowing between electrodes in two boreholes with constant voltage excitation. Note the data shows characteristics of two conductive zones between the pair of boreholes.

Another example of the cross-borehole injected electric current is shown in Figure 6, where one borehole intersects an ore zone, while the other borehole passing this zone at a distance. We can see that for the borehole intersects the ore zone, large electric current is observed for electrodes within certain depth range. For other borehole passing the ore at a distance, the ore zone shadow is visible from the injected electric current.

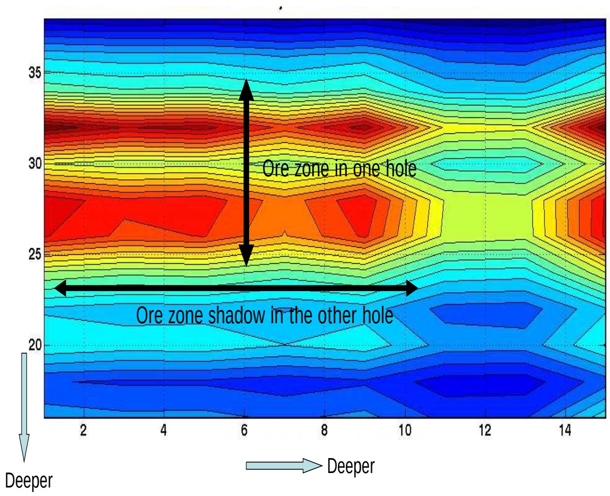


**Figure 6:** Electric current flowing between electrodes in two boreholes with constant voltage excitation. One borehole intersects an ore zone, while the other borehole passing this zone at a distance.

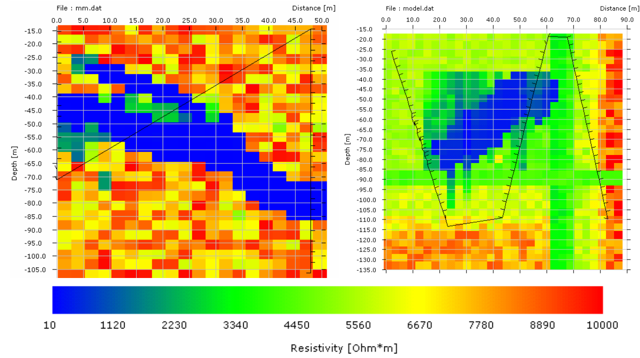


**Figure 7:** Two examples of BRT models derived from 2D tomographic inversions from the Sudbury area. The borehole traces are projected onto the 2D plane, where the resistivity structure is inverted. We assume the resistivity structure will not change in the direction perpendicular to the 2D plane.

## CROSS BOREHOLE RESISTIVITY TOMOGRAPHY (BRT)

We construct the BRT model by applying the following steps: (1) use VRP pseudo section to build a starting model at the two borehole locations; (2) perform inversion on VRP data only (use the starting model to constrain the inversion, no smoothness stabilizations applied); (3) build a starting model between two boreholes using the two resistivity inversion models derived from VRP data; (4) constrain the near borehole resistivities and let the tomography inversion adjust the resistivities in the central region; and finally (5) fine tune the tomography inversion model with geological / petrophysical constraints (where available). Two BRT models from two survey locations are shown in Figure 7, together with borehole traces.

## ACKNOWLEDGEMENTS

Funding for the borehole resistivity data acquisition was provided by Camiro with Xstrata Nickel Ltd., First Nickel Ltd. and CVRD Inco Technical Services Ltd participation. We are grateful to Alan King, Ben Polzer, Andrew Moores of Inco Technical Services Ltd., Daryl Ball of Xstrata Nickel Ltd. for insightful discussions. The equipment for this project was provided by Geoserve (www.geoserve.de). Michael Gräber is thanked for training and field support. The data interpretation software used for this demonstration project is developed by Geoserve Logging & Tomography.

## REFERENCES

Daniels, J.J., 1977, Three dimensional resistivity and induced-polarization modeling using buried electrodes, Geophysics, 42, 1006-1019.

Daniels, J.J. and Dyck, A., 1984, Borehole resistivity and electromagnetic methods applied to mineral exploration. IEEE Transactions on Geoscience and Remote Sensing, GE-22, 80-87.

Loke, M.H. and Barker, R.D., 1995, Least-squares deconvolution of apparent resistivity pseudosections, Geophysics, 60, 1682-1690.

Loke, M.H. and Barker, R.D., 1996, Rapid Least-squares inversion of apparent resistivity pseudosections by quasi-Newton method, Geophysical Prospecting, 44 (1), 131-152.

Mwenifumbo, C.,J., 1997, Electrical Methods for Ore Body Delineation, in: Proceedings of Exploration 97: Fourth Decennial International Conference on Mineral Exploration, A.G. Gubbins (edt.), 667-676.

Shima, H., 1992, 2D and 3D resistivity imaging reconstruction using cross-hole data, Geophysics, 55, 682-694.

Zhou, B. and Greenhalgh S. A., 2000, Cross-hole resistivity tomography using different electrode configuration, Geophysical Prospecting, 48 (5), 887-912.